Spooner, P. T., Robinson, L., Hemsing, F., Morris, P. J., & Stewart, J. (2018). Extended calibration of cold-water coral Ba/Ca using multiple genera and co-located measurements of dissolved barium concentration. *Chemical Geology*, *499*, 100-110. https://doi.org/10.1016/j.chemgeo.2018.09.012

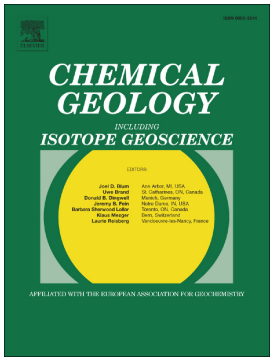

Extended calibration of cold-water coral Ba/Ca using multiple genera and co-located measurements of dissolved barium concentration

Peter T. Spooner, Laura F. Robinson, Freya Hemsing, Paul Morris, Joseph A. Stewart

PII: S0009-2541(18)30452-2
DOI: doi:10.1016/j.chemgeo.2018.09.012
Reference: CHEMGE 18905

To appear in: *Chemical Geology*

Received date: 18 September 2017
Revised date: 2 July 2018
Accepted date: 10 September 2018

Please cite this article as: Peter T. Spooner, Laura F. Robinson, Freya Hemsing, Paul Morris, Joseph A. Stewart , Extended calibration of cold-water coral Ba/Ca using multiple genera and co-located measurements of dissolved barium concentration. Chemge (2018), doi:10.1016/j.chemgeo.2018.09.012

Extended calibration of cold-water coral Ba/Ca using multiple genera and co-located measurements of dissolved barium concentration

Peter T. Spooner[a,1,*], Laura F. Robinson[a], Freya Hemsing[b,c], Paul Morris[a,2], Joseph A. Stewart[a]

[a]*School of Earth Sciences, University of Bristol, Queens Rd., Bristol, BS8 1RJ, UK*
[b]*School of Earth Sciences, University of Oxford, South Parks Rd., Oxford, OX1 3AN, UK*
[c]*Institute of Environmental Physics, Heidelberg University, Im Neuenheimer Feld 229, 69120 Heidelberg, Germany*

Abstract

Biological productivity and ocean circulation are both important oceanographic variables that control the distribution of dissolved barium in the ocean interior ($[Ba]_{sw}$). The ability to accurately reconstruct $[Ba]_{sw}$ will provide key constraints on these processes in the past. The geochemistry of cold-water corals has the potential to unlock paleoceanographic records at spatial and temporal resolutions not available using other sedimentary archives. Previous studies have suggested that the Ba/Ca ratio of coral skeletons is linearly related to $[Ba]_{sw}$. However, these efforts have used a limited number of species, sparse global seawater databases, or have not explicitly measured the Ba/Ca ratio. Here we investigate the Ba/Ca ratio in a well-constrained set of cold-water scleractinian (aragonitic) corals as a proxy for $[Ba]_{sw}$, using 58 specimens from 7 coral genera along with co-located measurements of $[Ba]_{sw}$. We find that traditional chemical cleaning procedures do not significantly affect the Ba/Ca ratio of cold-water coral skeletons, allowing rapid sample throughput. We also determine that intra-sample variation in Ba/Ca ratios can be reduced by using larger sample sizes (e.g. 20 mg). By combining our results with existing data, we find that cold-water coral Ba/Ca is linearly related to $[Ba]_{sw}$ according to the relationship: Ba/Ca µmol/mol = [0.15 ± 0.02] [Ba_{sw} nmol/kg] + [2.5 ± 1.4], (R^2 = 0.7). We observe no species-specific 'vital effects' in cold-water coral Ba/Ca ratios, but site-specific effects could be a factor. Nevertheless, our results highlight the potential of Ba/Ca in cold-water corals to reconstruct biological and physical changes in the ocean interior.

Keywords: Cold-water coral, Coral, Barium, Ba/Ca, Calibration

* Corresponding author: p.spooner@ucl.ac.uk
[1]Present Address: Department of Geography, University College London, Gower Street, London, WC1E 6BT, UK
[2]Present Address: Department of Nuclear Sciences and Applications, International Atomic Energy Agency, Monaco

1. Introduction

The dissolved barium concentration in seawater ($[Ba]_{sw}$) has a nutrient-like profile (Chan et al., 1977; Jeandel et al., 1996). Depletions of $[Ba]_{sw}$ in the upper mixed layer are a result of adsorption/absorption of Ba onto organic particulates (Cardinal et al., 2005; Collier and Edmond, 1984; Hoppema et al., 2010; Jacquet et al., 2008, 2007; Sternberg et al., 2005). Ba is also removed from deeper waters (100-1000 m) as a result of barite formation in and around aggregates of sinking organic matter, and is released back into the water column following remineralisation (Bishop, 1988; Cardinal et al., 2005; Dehairs et al., 1980; Dymond et al., 1992; Ganeshram et al., 2003; Jacquet et al., 2007; Stroobants et al., 1991; van Beek et al., 2009). Collectively, these effects cause the deep ocean to be enriched in $[Ba]_{sw}$ relative to the surface. Therefore, knowledge of past dissolved barium concentration in the deep ocean may provide insight into paleo-ocean productivity and circulation.

Increasing attention is being paid to cold-water corals as paleoceanographic archives, with numerous elemental and isotopic ratios being tested as proxies for past ocean conditions (Robinson et al., 2014). Two key advantages of using scleractinian (aragonitic) corals for deep sea research are: 1) the ability to precisely date their skeletons using uranium (U)-series methods (Cheng et al., 2000), and 2) their wide geographic and bathymetric distribution, spanning multiple water masses and ocean basins (Roberts, 2006).

The Ba/Ca ratio in deep- and shallow-dwelling scleractinian coral skeletons (aragonite) has been shown to reflect the concentration of dissolved Ba in seawater ($[Ba]_{sw}$) (Anagnostou et al., 2011; Gonneea et al., 2017; Hemsing et al., 2018; LaVigne et al., 2016). This result is similar to findings for calcitic corals, foraminifera and inorganic aragonite (Dietzel et al., 2004; Hönisch et al., 2011; LaVigne et al., 2011; Lea and Boyle, 1993), and appears to be robust despite a range of vital effects that occur during coral growth (e.g. Adkins et al., 2003; Case et al., 2010; Gaetani and Cohen, 2006; Sinclair et al., 2006; Spooner et al., 2016b). These vital effects are often most apparent between two microstructures of the coral skeleton, centres of calcification (COCs) and fibrous aragonite thickening deposits (TDs) (Fig. 1). Yet, limited data suggest that, in cold-water corals, the Ba/Ca ratio is largely invariant between COCs and TDs (Anagnostou et al., 2011). Thus, whilst the relative proportions of these microstructures in a sample can hamper the use of many traditional paleoceanographic proxies such as Mg/Ca (Gagnon et al., 2007), the Ba/Ca ratio may be

less affected. However, several issues remain to be addressed to allow the use of Ba/Ca as a tracer for past $[Ba]_{sw}$.

Previous studies have highlighted the impact of chemical cleaning on elemental ratios in biogenic carbonates, results that may be ascribed to either removal of contaminants (such as adsorbed metals, organics or Fe-Mn oxides) and/or partial skeletal dissolution during acid leaching and reductive steps (Barker et al., 2003; Cheng et al., 2000; Mitsuguchi et al., 2001; Montagna et al., 2014; Rosenthal et al., 2004; Shen and Boyle, 1988; van de Flierdt et al., 2010; Watanabe et al., 2001). Studies have generally found no impact of cleaning on coral Ba/Ca (Holcomb et al., 2015; Tudhope et al., 1996), but the subject warrants further testing to develop a robust and reproducible methodology for cold-water corals.

Thus far, there has been no concerted study explicitly measuring Ba/Ca ratios in multiple species of cold-water coral with dedicated measurements of $[Ba]_{sw}$, leaving questions as to the impact of species- (or genus-) specific, and site-specific vital effects. Here we present a new calibration of cold-water coral Ba/Ca versus $[Ba]_{sw}$ based on a recently-collected sample set from the Atlantic and Southern Ocean (SO)(Chen et al., 2015; Spooner et al., 2016b). Samples in this collection are precisely located and many were alive upon collection. We present data from 58 individual specimens, representing 7 different coral genera from two different ocean settings. We further improve on previous studies by calibrating the coral Ba/Ca ratios against co-located $[Ba]_{sw}$ and by assessing the impacts of using different cleaning procedures and sample sizes on cold-water coral Ba/Ca ratios. Furthermore, we use measurements of other local seawater properties (temperature, salinity, nutrients, oxygen concentration and carbonate chemistry) to assess the impact of these auxiliary factors on the Ba-calibration and its potential paleoceanographic utility.

2. Methods

2.1. Coral sample collection and dating

Coral skeletons were collected during three cruises (NBP0805, NBP1103 and LMG0605) to the SO (Drake Passage), one cruise (JC094) to the tropical Atlantic Ocean (Fig. 2), and one cruise to the Reykjanes Ridge (CE0806) (Burke and Robinson, 2012; Chen et al., 2015; Jones et al., 2014; Spooner et al., 2016b). Note that samples from the Reykjanes Ridge were only included in the cleaning and sample-size experiments (Section 2.4) and not the calibration because of a lack of $[Ba]_{sw}$ at the depths of the samples in this study. Samples for

the calibration were either collected alive using a Remotely Operated Vehicle (ROV, tropical Atlantic samples, n = 33) or were sub-fossil specimens (i.e. dead) with skeletons <1 ka old, collected using dredges and trawls (Drake Passage samples, n = 25). The majority of dead sample ages were determined via U-series isotope dilution solution multi-collector inductively-coupled plasma mass spectrometry (MC-ICPMS) (Burke and Robinson, 2012) and the remainder by reconnaissance radiocarbon/U-series dating (Burke et al., 2010; Burke and Robinson, 2012; Margolin et al., 2014; Spooner et al., 2016a) (Table S1).

Sample depths ranged from 210 to 2500 m (Table S1). Sample locations using dredges and trawls are listed as the mean depth, latitude and longitude for each collection event. Drake Passage genera included *Balanophyllia*, *Caryophyllia*, *Desmophyllum* and *Flabellum*. Tropical Atlantic genera included *Caryophyllia*, *Dasmosmilia*, *Enallopsammia* and *Javania*. With the exception of *Enallopsammia* (a colonial coral), these are all solitary, scleractinian (aragonitic) corals (a single coral polyp with its own skeleton, typical morphological features shown in Fig. 1) (Cairns and Kitahara, 2012). Thus far, *Desmophyllum dianthus* has been the most commonly used solitary cold-water solitary coral in paleoceanographic studies (e.g. Burke and Robinson, 2012; Thiagarajan et al., 2014). It has an attached base but lacks a columella or pali (Fig. 1). Corals from the genera *Javania* and *Flabellum* also have these characteristics, but *Javania* has a pedicel thickened with successive layers of aragonite. *Dasmosmilia* is also attached and has a rudimentary columella. *Balanophyllia* corals have a highly porous outer thecal layer, which often becomes infilled by secondary carbonate minerals. The polyps of the colonial coral *Enallopsammia* tend to be small, housed within a branching porous skeleton.

2.2. Dissolved Ba and other seawater properties

Water samples collected during the tropical Atlantic JC094 cruise have been analysed for $[Ba]_{sw}$ previously (Bates et al., 2017). These water samples were from three locations across the Atlantic: Carter Seamount (JC094-CTD002), Vema Fracture (JC094-CTD005) Zone and Vayda Seamount (JC094-CTD006) (Fig. 3). These three sites had very similar $[Ba]_{sw}$ profiles suggesting that they are representative of the tropical Atlantic region. We therefore used these profiles to estimate $[Ba]_{sw}$ for the remaining tropical Atlantic sample sites (Fig. 1).

Water collected during the Drake Passage NBP1103 cruise was analysed for $[Ba]_{sw}$ at the University of Oxford as part of a companion study on barium isotopes (Hemsing et al., 2018).

Samples were taken from Burdwood Bank (NBP1103-CTD021) and Sars Seamount (NBP1103-CTD100) (Fig. 2 and 3).

Temperature (T) and salinity (S) (Fig. 3; Table S2) were measured at or near each coral collection site and compared with ocean atlas data (Levitus and Boyer, 1994) to estimate the variability of these parameters at each sample site, following the methods in Spooner et al. (2016b).

For cruise JC094, major nutrients (nitrate, phosphate, silicic acid; Table S2) were measured at the University of Plymouth in seawater samples frozen at -20 ^{o}C during the cruise (Bates et al., 2017; Robinson, 2014). During the Southern Ocean cruises, filtered seawater samples were also frozen at -20 ^{o}C before nutrient concentrations were measured at Woods Hole Oceanographic Institution Nutrient Analytical Facility (e.g. Hendry et al., 2010).

During NBP0805 and NBP1103, dissolved oxygen concentrations (ml/l) were measured with a Sea-Bird Electronics-43 dissolved oxygen sensor attached to the CTD carousel. Data were converted to µmol/l based on the standard conversion used in the Sea-Bird Electronics software. During JC094, dissolved oxygen concentration was also measured using a Sea-Bird Electronics-43 sensor. Shipboard measurements were also performed on every water sample using Winkler titrations to ensure a good sample calibration of the Sea-Bird sensor (Carritt and Carpenter, 1966; Robinson, 2014).

Carbonate chemistry parameters (total alkalinity and dissolved inorganic carbon) for the tropical Atlantic sites were measured by the UK Ocean Acidification Research Program Carbonate Chemistry Facility at the National Oceanography Centre (NOC), Southampton, in seawater samples that were collected close to the coral collection sites (Robinson, 2014). For the Southern Ocean sites we made use of a recent carbonate system re-analysis to estimate the parameters of interest (Bostock et al., 2013). We used estimates of the alkalinity and dissolved inorganic carbon from the re-analysis at the grid location and depth closest to each sample site and the measured temperature, salinity and nutrient data from each site (measured during the sample collection cruises) to estimate the remaining carbonate system parameters using the CO2SYS program (Pierrot et al., 2006).

Water sampling was typically carried out at ~12 depths per location. Therefore, we linearly extrapolated measurements from the depths closest to coral collection sites to estimate the water properties at those depths (Table S2).

2.3. Sample preparation

Immediately after collection from the seabed, sub-fossil (i.e. dead) coral skeletons were rinsed with fresh water. Live-collected corals were bleached to remove external organic tissue, followed by freshwater rinses of the skeletons. All skeletons were then dried at room temperature. Approximately 20 mg of each coral was cut using a hand-held diamond saw. Samples were generally cut from the upper portion of the skeleton and included portions of both thecal and septal material (Fig. 1, Table S1). Relative proportions of COCs and TDs were not monitored. For the genus *Enallopsammia*, samples were taken from both the tips of branches (i.e. polyp material) or the branches themselves. Each subsample was physically cleaned by gently milling the surfaces with the flat of the diamond saw to remove visible ferro-manganese crusts (for some sub-fossil specimens) and/or altered/chalky carbonate, or possible organic residues on live-collected specimens. The porous outer skeleton of all *Balanophyllia* corals was removed as much as possible. Samples were then ultrasonicated (US) in 18.2 MΩcm water (MQ) for 15 minutes to remove particulates introduced during the cutting and milling, rinsed with MQ and dried at room temperature.

Dry coral samples were placed in acid-cleaned Teflon vials for storage and dissolution. On the day of analysis, samples were dissolved in 50 µl concentrated super-pure (s.p.) HNO_3 and then diluted with 1.95 ml 0.5 M s.p. HNO_3. In preparation for ICPMS measurement, aliquots of each sample were further diluted into acid-cleaned Teflon autosampler vials to obtain solutions with Ca concentrations ([Ca]) of ~2.5 mM, in 1.5 ml of 0.5 M s.p. HNO_3. Dilutions were doped to 4 ppb In. Full procedural blanks were prepared in the same way as the samples.

2.4. Cleaning and sample size experiments

Cleaning tests were carried out on large aliquots of 15-20 mg taken from two powdered samples of sub-fossil coral. One sample (CE0806-Dr-18-1, Reykjanes Ridge) was ~110 ka old with an extensive, black ferro-manganese crust (Spooner et al., 2016a). The other sample (NBP1103-TB10-Dp-3, Drake Passage) was <1 ka old and lacked such crusts.

We used standard cleaning procedures designed to remove adsorbed metals, ferro-manganese crusts and organic material, adapted from procedures used during U-series and trace metal analysis of cold-water corals (Burke and Robinson, 2012; Cheng et al., 2000;

Shen and Boyle, 1988). The cleaning steps (each followed by three MQ water rinses) were as follows, with: Every coral underwent shipboard freshwater rinses, followed by lab-based removal of ferro-manganese crusts and visibly altered aragonite with a diamond disc. This physical clean was followed by 15 min ultrasonication (US) in MQ to remove adsorbed metals and other contaminants introduced during sample preparation and step 1 (Mitsuguchi et al., 2001). After this step, large pieces of coral aragonite were cut and powdered in a pestle and mortar for further cleaning, and different aliquots of the powder were then rinsed with MQ and subjected to between none and all of the following chemical cleaning steps: 1) 15 min US in an oxidising, 1:1 mixture of 30 % H_2O_2 and 1 M NaOH, heated to ~60 ^{o}C to remove organics; 2) 2 min rinse in a 1:1 mixture of 1 % $HClO_4$ and 30 % H_2O_2, to vigorously remove remaining organics (Cheng et al., 2000); 3) step 2 repeat; 4) 1 min US in 0.2 % (by mass) HNO_3, to leach remaining surficial contaminants; 5) step 3 repeat; 8) 20 min US in a reducing solution, made by mixing 20 ml of solution A (see below) with 20 ml NH_4OH (conc.) and 1.5 ml hydrazine, to remove remaining metal-rich oxides. Solution (A) was made by dissolving 30 g citric acid powder into 250 ml of milli-q and adding 250 µl NH_4OH (conc.).

In addition to the effects of cleaning, it is possible that intra-skeletal variability could result in scatter in a Ba/Ca versus $[Ba]_{sw}$ calibration. Therefore, we carried out two experiments to test the effect of sample size on measurement reproducibility. The coral NBP0805-TB04-Big Beauty was collected from the Drake Passage and is included in the calibration study. Ten solid subsamples were cut each of 5 mg, 10 mg, 20 mg and 40 mg. The coral CE0806-Dr04A-1 was collected during a cruise to the Reykjanes Ridge, Iceland (CE0806). For this coral, five subsamples were taken each of 5 mg, 10 mg, 20 mg and 40 mg. Samples were prepared as described above but were not chemically cleaned given the results of the cleaning experiments (Section 3.1). Ba/Ca was measured in each sample as described below and the reproducibility calculated for each size class.

2.5. Measurement procedures

A multi-element standard (CrIME) containing Li, B, Mg, P, Ca, Fe, Mn, Sr, Ba and U was gravimetrically prepared by mixing single-element solutions supplied by High-Purity Standards Incorporated. CrIME element/Ca ratios were calculated based on the mass, density, elemental concentration (in µg l^{-1}) and impurity data (supplied with the certification for each solution) of each single element solution, and were designed to reflect average cold-water scleractinian coral values found in the literature (final gravimetric Ba/Ca = 7.64 ±0.05 µmol/mol). On the day of analysis, the standard was diluted into sample vials to a concentration of ~2.5 mM Ca.

Samples were measured in the Bristol Isotope Group (BIG) using a ThermoFinnigan Element 2 ICPMS following standard methods (e.g. Rae et al., 2011; Rosenthal et al., 1999). Prior to running full trace metal analysis, sample Ca concentrations ([Ca]) were checked by comparison with four solutions of varying [Ca] (0.5 mM, 1 mM, 2.5 mM and 5 mM). If necessary, samples were re-diluted to ensure that their [Ca] was within 10 % of the multi-element standard (typically ~2.5 mM [Ca]). The majority of the samples were matched to the [Ca] of the CrIME standard to within 2 %.

During sample analysis ^{43}Ca, ^{48}Ca, ^{115}In and ^{137}Ba were measured in low resolution. ^{55}Mn, ^{56}Fe and ^{115}In were measured in medium resolution. ^{115}In was used to normalise the medium resolution measurements to obtain Mn/Ca and Fe/Ca. Each sample acquisition took 3.5 minutes. CrIME was run at the start and end of the sequence and after every two samples, and was used to calculate elemental ratios (El/Ca_{sample}) from counts per second data using the approach of (Rosenthal et al., 1999).

Procedural blanks were measured before and after each standard measurement, the averages of which were subtracted from measured standard/sample signal intensities before calculation of elemental ratios. Typical blank intensities were 0.1 % for ^{137}Ba and 0.01 % for ^{43}Ca and ^{48}Ca.

Element/calcium ratios were calculated using both ^{43}Ca and ^{48}Ca, and the results were compared for each sample run. There was no significant difference between these two calculation methods for any of the samples. Reported elemental ratios (Table S1) are the mean of the ratios calculated using ^{43}Ca and ^{48}Ca.

Fe/Ca and Mn/Ca measurements were used to assess potential contamination from residual ferro-manganese crusts not removed by physical cleaning.

Three consistency standards were used to determine measurement accuracy and precision: 1) the coral powder JCp-1 (Okai et al., 2002); 2) an in-house cold-water coral powder (Dr18-1p) and 3) a second multi-element solution (PTS-1), prepared similarly to CrIME. JCp-1 has been the subject of an interlaboratory calibration exercise for elemental ratios (Hathorne et al., 2013). The mean Ba/Ca value measured for JCp-1 in this study (6.96 ± 0.08 µmol/mol 2 S.E., n = 13) was less than the average value of 7.465 ± 0.655 µmol/mol in Hathorne et al. (2013), but the results are within the robust interlaboratory 2 S.D. We also measured Ba/Ca in an in-house mixed solution standard BSGS (Ni et al., 2007; Rae et al., 2011). The Ba/Ca

ratio we measured was within 2 % of those studies. To facilitate comparison with Hemsing et al. (2018) (who measured Ba/Ca of JCp-1 = 7.94 ± 0.22 µmol/mol), we here adjust our respective data sets by factors required to obtain JCp-1 Ba/Ca = 7.465 µmol/mol (i.e. x1.073 in this study, and x0.940 for data from Hemsing et al. (2018)).

Based on measurements of PTS-1 (83 measurements) and Dr18-1p (12 measurements), the 12-month Ba/Ca reproducibility was ± 1.6 % 2 standard deviations (2 S.D.).

3. Results

3.1. Cleaning experiments and Fe/Ca

The maximum difference in Ba/Ca between powder aliquots cleaned to different extents was 2.6 % (Fig. 4, Table 1). NBP1103-TB10-Dp-3 did not show any consistent change in Ba/Ca with progressive cleaning. However, the Ba/Ca ratio in CE0806-Dr18-1 decreased by 2.6 % after the oxidative/perchloric acid steps. This difference in results for the two corals may be due to relatively high Fe/Ca ratios in CE0806-Dr18-1, possibly indicating contamination by non-carbonate phases (e.g. ferro-manganese oxides) that were removed during the oxidative cleaning (Cheng et al., 2000). The two aliquots limited to physical cleaning and water washes had Ba/Ca ratios of 6.83-6.85 µmol/mol and Fe/Ca ratios of 40-50 µmol/mol. After cleaning with oxidising solution and perchloric acid, Ba/Ca ratios fell to 6.70 µmol/mol and Fe/Ca ratios fell to <20 µmol/mol.

In agreement with other studies, our cleaning results for these corals show that, even in the presence of relatively high Fe concentration (i.e. potentially high volumes of contaminating phases), the effect of chemical cleaning on coral Ba/Ca is small (Holcomb et al., 2015). It has also been shown that such chemical cleaning can lead to selective dissolution of carbonate material (e.g. Barker et al., 2003), which could have inconsistent impacts on measured skeletal geochemistry.. We therefore did not clean samples used for the calibration beyond the basic mechanical cleaning. In order to account for the potential impact of contaminating phases outlined above, we use Fe/Ca ratios to exclude potentially contaminated samples from the analyses.

A common limit applied to foraminifera to exclude contaminated carbonate is that Fe/Ca should be <175 µmol/mol (e.g. Bice et al., 2005; Lea et al., 2005). However, given the results outlined above we take a conservative approach to identifying contamination by

excluding samples with Fe/Ca >40 µmol/mol from the analyses. Two measurements were excluded in this way (Table S1). The mean Fe/Ca ratio of all samples with Fe/Ca <40 µmol/mol was 3 µmol/mol.

3.2. Sample size experiments

In both corals analysed for different size samples, the reproducibility of Ba/Ca (2 S.D.) was better than 10 % for all size categories and generally improved with increasing sample size (Fig. 5). For the 20 mg category, reproducibility was 7 % for NBP0805-TB04-Big Beauty and 6 % for CE0806-Dr04A-1. These values are greater than the variability in the cleaning experiments because subsamples were distinct (i.e. not powdered and mixed) and represent different areas of the skeleton. Based on the results of this experiment, we chose used 20 mg samples from each coral in the calibration as a compromise between reproducibility and sample limitation in smaller specimens. Such samples are large compared to previous work (e.g. laser ablation) and given our results may be expected to decrease scatter in the calibration. Using these methods, our data suggest that intra-skeletal variability could introduce scatter of ~7 % into the Ba/Ca values.

3.3. Calibration of cold-water coral Ba/Ca versus $[Ba]_{sw}$

We find that coral Ba/Ca is linearly related to $[Ba]_{sw}$ (Fig. 6). After adjustment by the factor required to bring our JCp-1 data into agreement with Hathorne et al. 2013 (i.e. x1.073), a linear least squares regression of the coral measurements (average for each specimen) in this study suggests the calibration equation: Ba/Ca µmol/mol = [0.12 ± 0.02] [Ba_{sw} nmol/kg] + [4.72 ± 1.08], $R^2 = 0.79$, $p < 0.01$. The regression results in prediction errors (uncertainty of predicting $[Ba]_{sw}$ based measured Ba/Ca in corals) of ~14- nmol/kg (95 % confidence) (Fig. 7). Regressing the same data using a weighted bivariate regression approach (Cantrell, 2008; York et al., 2004), results in a slightly steeper slope and lower intercept than obtained using the standard least squares fit: Ba/Ca µmol/mol = [0.15 ± 0.02] [Ba_{sw} nmol/kg] + [2.86 ± 1.09], with a goodness of fit parameter equal to 2.8 (Cantrell, 2008), indicating that the model has not fully captured the data variability. The regression models suggest that the standard least squares fit likely represents a minimum of the Ba/Ca versus $[Ba]_{sw}$ slope and is therefore the more conservative choice for interpreting paleo data. We also note that the lines are within uncertainty of one another and do little to change the data interpretation here. Hence, for simplicity, discussion (below) is based on the least squares calibration. We note that, even without standard-based adjustment of the data, the calibration has a significantly positive y-intercept.

Residuals are consistent with a normal distribution according to a Kolmogorov-Smirnov (K-S) test for normality. Residuals are not related to $[Ba]_{sw}$, suggesting that a linear fit to the data is appropriate for the data range covered. The numbers of samples from individual genera are small (3 to 20), but further genus-specific K-S normality tests indicate that the residuals for each coral genus are consistent with normal distributions. Applying t-tests to the residuals of these genera indicates that no genus has a mean residual that is significantly different to that of any other genus, suggesting that genus-specific vital effects are not important for skeletal Ba/Ca ratios.

4. Discussion

4.1. Covariance of seawater properties

Our coral data indicates that $[Ba]_{sw}$ can explain 79 % of the variance in coral Ba/Ca. The residuals of the regression are not significantly correlated with temperature, salinity, carbonate ion concentration, nutrient concentration or oxygen concentration. For corals living within the thermocline (tropical Atlantic *Dasmosmilia*), it is possible that seawater properties changed over the lifetime of the corals. However, we largely discount this factor as a dominant driver of coral Ba/Ca scatter, as similar variability occurs in samples from the same locations and depths, suggesting that the residual spread of data is more likely to be explained by intra-skeletal variability in the Ba/Ca ratio.

Superficially, coral Ba/Ca appears to be related to in-situ T and S (Fig. 8). However, these relationships are clearly dominated by the covariation between $[Ba]_{sw}$, T and S in the water column. For example, while coral Ba/Ca and T appear correlated in Figure 8b, the correlation is not linear. Rather, the Ba/Ca ratios of Drake Passage corals change more rapidly with T than those from the tropical Atlantic. This pattern closely matches the relationship between $[Ba]_{sw}$ and T across the sites (Fig. 8a), indicating that the correlation between Ba/Ca and T is driven by the dependence of Ba/Ca on $[Ba]_{sw}$. The same argument can be made for the correlation between Ba/Ca and salinity (Figures 8c and 8d).

These inferences are supported by a recent culturing study that found strong dependence of warm-water coral Ba/Ca on $[Ba]_{sw}$, and relatively minor T dependence (Gonneea et al.,

2017). However, the results of this culturing study and other experimental studies of abiogenic aragonite growth reveal that low temperatures are associated with higher aragonite Ba/Ca ratios, showing that temperature does have some effect on coral Ba/Ca ratios (Dietzel et al., 2004; Gaetani and Cohen, 2006). Because the corals from our study from areas with high $[Ba]_{sw}$ (Drake Passage) were also living in low temperature environments, the temperature effect described above would increase the slope of our calibration. Based the results of Gonneea et al. (2017) and Dietzel et al. (2004) and assuming a low-end partition coefficient between aragonite and seawater of 1.5 ($D_{Ba/Ca}$, Section 4.4), the 8 ^{o}C temperature increase across our sites would result in a small but measurable 1 µmol/mol decrease in coral Ba/Ca. This could account for around 14 % of the total change in Ba/Ca, with the rest attributed to changes in $[Ba]_{sw}$. However, both of the experiments cited above were conducted at temperatures above those experienced by our coral samples (10 – 50 ^{o}C), and disagree in the magnitude of the temperature effect with another study conducted at even higher temperature (Gaetani and Cohen, 2006), highlighting the need for further controlled experiments to assess the impact of temperature on Ba/Ca, particularly in cold-water specimens.

4.2. Comparison to existing $[Ba]_{sw}$ calibrations

The cold-water coral Ba/Ca versus $[Ba]_{sw}$ calibration using data from this study suggests a well-defined, linear relationship, despite the inclusion of samples from different sites and coral genera. However, there remain some discrepancies between these new calibration data and those presented in other studies (Fig. 9).

In a study on barium isotopes (Hemsing et al., 2018), Ba/Ca ratios were obtained as an ancillary product in a sample set that included the major sample locations in this study, and also Iceland (Fig. 9). A total of 15 coral specimens (different subsamples) were measured by both studies. After adjusting the data each study by the factors outlined in Section 2.5, the Ba/Ca ratios of these 15 shared samples do not differ by more than 10 % between the studies, in line with the expected intra-skeletal variability found in our sample size experiments.

Combined (with averages taken for replicate samples), the data from the two studies suggest the relationship: Ba/Ca µmol/mol = [0.15 ± 0.02] [Ba_{sw} nmol/kg] + [2.5 ± 1.4], R^2 = 0.70, $p < 0.01$ (Fig. 9). This relationship has a higher slope and lower intercept than found with the corals measured only in this study. However, the Ba/Ca ratios for corals from the same sample sites agree very well between the two studies (Fig. 9). The discrepancy

between the regression models arises because every sample from Iceland (Hemsing et al. 2018) has relatively low Ba/Ca compared to corals from the other sites with similar $[Ba]_{sw}$, even though they represent a mixture of three different species (Fig. 9). This finding suggests that there could be a site-specific effect acting on these corals (Section 4.3).

The only other study to examine Ba/Ca in cold-water corals used laser ablation analyses in a sample set mainly based on museum specimens (Anagnostou et al., 2011). The laser ablation was used to target TDs in *D. dianthus*. This study found the relation: Ba/Ca µmol/mol = [0.09 ± 0.05] [Ba_{sw} nmol/kg] + [2.9 ± 3.4]. The scatter in this data set is relatively large (i.e. a zero or non-zero intercept cannot be established), with some of the corals falling close to our calibration, while other Ba/Ca ratios plotting up to 4 µmol/mol below (Fig. 9). The relatively low and scattered laser ablation Ba/Ca results may stem from analytical artefacts, uncertainty in $[Ba]_{sw}$, site-specific effects (as above), or micro-structure coral heterogeneities. We consider the first of these reasons to be the main factor. Although estimates of $[Ba]_{sw}$ were not taken from co-located seawater measurements (as in our current study), uncertainties beyond 10 nmol/kg seem unlikely. Samples were collected from a wider variety of sampling sites (Atlantic, Pacific, Southern Ocean), so that low Ba/Ca ratios cannot be ascribed to any particular location. In addition, the Ba/Ca of samples from Burdwood Bank at ~400 m depth that we measure (~12 µmol/mol) is 40 % higher than the Ba/Ca measured in a similar sample by Anagnostou et al., (2011) (8.48 µmol/mol), suggesting that effects other than sample site-specific effects are affecting the data. In the one coral sample where both COCs and fibrous aragonite TDs were targeted by laser work, it was suggested that these microstructures do not have very different Ba/Ca ratios (Anagnostou et al., 2011), although micron-scale heterogeneities cannot be completely ruled out. While laser-ablation techniques offer elemental mapping capabilities at unprecedented spatial resolution, there are clear analytical draw-backs to this approach in the form of variable matrix effects and a lack of suitably homogenous, well-characterised, LA-ICP-MS carbonate reference material to permit direct data comparison between laboratories (Limbeck et al., 2015). Thus, while the results of Anagnostou et al. (2011) represent an important first step towards ground-truthing the proxy and in general support the proposed sensitivity (slope) of coral Ba/Ca to $[Ba]_{sw}$ in our study, we likely cannot directly compare absolute values between the two studies.

Ba/Ca measurements in the warm-water scleractinian corals *Porites lobata*, *Pavona gigantea* and *Pavona clavus* were compared to $[Ba]_{sw}$ measured over the course of a year in the Gulf of Panama (LaVigne et al., 2016). Taking these data together they give the relationship: Ba/Ca µmol/mol = [0.99 ± 0.02] [Ba_{sw} nmol/kg] + [1.0 ± 1.2]. In a recent study, Ba/Ca was measured in cultured specimens of the warm-water scleractinian *Favia fragum* at

three different temperatures (Gonneea et al., 2017). Without forcing the regression line through the origin, data from three corals grown at 27.7 ^{o}C suggest a calibration line of: Ba/Ca µmol/mol = [0.17 ± 0.004] [Ba_{sw} nmol/kg] - [1.0 ± 1.0].

With respect to the cold-water calibrations we present here, the corals from LaVigne et al. (2016) show a similar Ba/Ca sensitivity to $[Ba]_{sw}$, but all have Ba/Ca values that are around 4 µmol/mol lower for similar $[Ba]_{sw}$. Based on the temperature effect discussed above, around 2 µmol/mol of this difference could be explained by the relatively warmer temperatures experienced by these tropical corals. However, despite also being grown in warm water, the Ba/Ca value of the cultured warm-water coral *Favia fragum* specimen grown at $[Ba]_{sw}$ of 79 ± 23 nmol/kg is closer to that which would be expected from our calibration (Gonneea et al., 2017), again pointing to the need for more culturing experiments to better define the culture calibration at natural $[Ba]_{sw}$ concentrations, to determine whether there is some difference in Ba uptake by warm- and cold-water corals or non-linearity in the calibration at extremely low $[Ba]_{sw}$ values.

4.3. Genus- and site-specific calibrations

As well as potential bias in the calibration related to temperature change, additional Ba/Ca variability may stem from genus- and/or site-specific effects. Indeed, we have shown above that the combined calibration between this study and Hemsing et al. (2018) reveals a potential site-specific effect observed in the Icelandic corals.

Species-specific effects may arise because of differences in coral physiology or calcification (e.g. Spooner et al., 2016b). However, a standard linear least squares calibration based only on *Caryophyllia*, the genus with the most samples (n = 24, including Hemsing et al. 2018) and greatest range in $[Ba]_{sw}$ (~50 nmol/kg) returns a line statistically identical to the overall regression: $Ba/Ca_{Caryophyllia}$ µmol/mol = [0.13 ± 0.03] [Ba_{sw} nmol/kg] + [3.6 ± 1.8], R^2 = 0.79, $p < 0.01$. This result, combined with the genus-specific residuals detailed in Section 3.3, suggests that genus/species-specific effects are minor and that the calibration may be applicable to all cold-water scleractinia.

However, the possibility of site-specific effects on coral Ba/Ca complicates this picture. Unfortunately, the small range in $[Ba]_{sw}$ experienced by the Icelandic samples precludes defining a calibration line for that site. Combining the data from this study and from Hemsing et al. (2018) (as above, i.e. averaging data for replicated samples) and excluding the Iceland samples, we obtain the relationship: Ba/Ca µmol/mol = [0.12 ± 0.02] [Ba_{sw} nmol/kg] + [4.4 ±

1.0], R^2 = 0.78, p < 0.01, statistically the same as that using only the data in this study. Samples from the tropical Atlantic give the regression line: Ba/Ca µmol/mol = [0.085 ± 0.04] [Ba_{sw} nmol/kg] + [6.3 ± 2.3], R^2 = 0.28, p < 0.01. The slope and intercept of this line are within error of those for the overall regression, but the line is naturally more poorly fit due to the small range in $[Ba]_{sw}$ of ~25 nmol/kg. This relationship also represents all the data for live-collected specimens, indicating that the overall result is robust with or without inclusion of sub-fossil material. A regression through the Southern Ocean samples gives a similar regression over a wider range of $[Ba]_{sw}$: Ba/Ca µmol/mol = [0.10 ± 0.03] [Ba_{sw} nmol/kg] + [6.54 ± 2.12], R^2 = 0.68, p < 0.01. The similarity of both of these lines with the overall regression again suggests that the results from Iceland are anomalous.

Cooler temperatures in Icelandic waters would serve to slightly increase coral Ba/Ca relative to low latitude sites. Therefore, a temperature effect alone cannot explain the low Icelandic Ba/Ca values. It could be that the measurements of $[Ba]_{sw}$ for the Iceland sites, taken in June, are not representative of the annual value, due to either substantial seasonal changes in export productivity or to the seasonal strength of Iceland-Scotland Overflow Water (Bower and Furey, 2017; Sundby et al., 2016). A further possibility is that the conditions for coral growth around Iceland impact coral calcification in other ways, perhaps by affecting growth rates or the relative proportions of different skeletal microstructures. These ideas are speculative and new measurement campaigns on other sample sites will be needed to explore the possibility of site-specific vital effects further.

4.4. $D_{Ba/Ca}$

The distribution coefficient $D_{Ba/Ca}$ for coral aragonite is the ratio of Ba/Ca in the aragonite structure to that of the water from which the aragonite precipitated: $D_{Ba/Ca}$ = (Ba/Ca_{coral}) / (Ba/Ca_{water}). $D_{Ba/Ca}$ >1 indicates that Ba is preferentially incorporated into the aragonite (as opposed to remaining in the water). To calculate $D_{Ba/Ca}$ for each coral here we make several assumptions. We must assume that the corals are: 1) calcifying from a fluid of seawater composition; 2) calcifying in an open system or else in a batch process in which the whole of each batch of fluid is used up; and 3) that the only source of Ba to the skeleton is from the seawater dissolved pool (i.e. if $[Ba]_{sw}$ = 0 then the coral skeleton Ba/Ca ratio would also be zero). We take a constant value for seawater calcium concentration of 1.03 mmol/kg (Nozaki, 1997), but given a salinity variation across our sample sites, we assume a 5 % uncertainty on this value.

Under these assumptions we calculate $D_{Ba/Ca}$ values between 1.5 and 2.8 (Fig. 10). However, the significantly positive y-intercept of our calibration (Section 3.3) shows that, either $D_{Ba/Ca}$ changes systematically across the sample set (Fig. 10), or that one or more of our assumptions are incorrect.

Our assumptions may be incorrect for several reasons. Firstly, the assumption that the calcification fluid is of purely seawater composition is likely invalid. The favoured model of coral calcification suggests that corals import Ca^{2+} ions into the fluid (thus changing Ba/Ca) at the expense of H^+ ions, in order to up-regulate the pH to the extent required to easily precipitate aragonite (e.g. Cohen and McConnaughey, 2003; McConnaughey, 1989). Secondly, the enclosed nature of the fluid likely precludes fully open-system behaviour, allowing batch fractionation processes to affect skeletal chemistry on microscales that would not be detectable using our bulk sampling methods (e.g. Case et al., 2010; Gaetani et al., 2011; Montagna et al., 2014). Thirdly, while not yet demonstrated for cold-water corals, the presence of Ba-rich, cleaning-resistant contaminating phases such as interstitial organics or barite has been suggested for some warm-water corals (Tudhope et al., 1996). Although we showed above that chemical cleaning has little effect on coral Ba/Ca ratios, it is unclear whether such phases would have been completely removed by our cleaning experiments.

Given these issues with calculation of D_{Ba} and the positive intercept of our calibration lines, calculating past $[Ba]_{sw}$ from cold-water coral Ba/Ca using any single estimate of D_{Ba} is not an appropriate approach. However, the empirical calibration model of Ba/Ca vs $[Ba]_{sw}$ suggested by our data appears to be robust, despite inclusion of different species and methodologies, and can therefore be used to estimate past $[Ba]_{sw}$.

5. Conclusions

We have investigated the applicability of the Ba/Ca proxy in cold-water corals for determining the concentration of dissolved barium in seawater ($[Ba]_{sw}$) using solution-based single collector inductively coupled plasma mass spectrometry. Combined with data from a companion study, coral Ba/Ca appears to be linearly related to $[Ba]_{sw}$ according to the relation: Ba/Ca µmol/mol = [0.15 ± 0.02] [Ba_{sw} nmol/kg] + [2.5 ± 1.4].

A lack of correlation of the residuals of the regression with other ocean variables and the minor effect of temperature suggest that $[Ba]_{sw}$ is the dominant driver of cold-water coral Ba/Ca, explaining up to 79 % of the variance. The slope of this relationship is the same as those found for warm-water corals in previous studies. However, for samples growing in waters with low $[Ba]_{sw}$ (< 70 nmol/kg), cold-water corals appear to have higher Ba/Ca ratios than their warm-water counterparts, by an amount that is greater than the expected effect of temperature alone. In addition, we find that sample site-specific effects may be important for cold-water coral Ba/Ca ratios, with samples from Iceland having consistently lower Ba/Ca ratios than those from the tropical Atlantic.

Our calibration data from a variety of sample sites and genera imply that Ba/Ca measurements in cold-water scleractinian corals can be used to reconstruct $[Ba]_{sw}$ in the past ocean. Cold-water coral Ba/Ca is therefore a promising addition in the paleoceanographer's tool kit that will provide constraints on productivity and ocean circulation in the past.

6. Acknowledgements

The authors would like to thank Dr Christopher Coath and Carolyn Taylor in the Bristol Isotope Group and Jamie Lewis for assistance with the mass-spectrometry set up. We would like to thank the science teams and crews of the JC094, NBP0805, NBP1103 and LMG0806 cruises for sample and water collection. We also thank Gideon Henderson and the Oxford University Department of Earth Sciences for hosting FH, and Eleni Anagnostou for helpful discussion. This work was supported by a National Environment Research Council (NERC) studentship to PTS, European Research Council (ERC), Leverhulme Trust and NERC [grant number NE/N003861/1] funds to LFR, and Deutscher Akademischer Austauschdienst (DAAD) and Heidelberg Graduate School for Fundamental Physics (HGSFP) awards to FH. Conflicts of interest: None.

7. References

Adkins, J.F., Boyle, E.A., Curry, W.B., Lutringer, A., 2003. Stable isotopes in deep-sea corals and a new mechanism for “vital effects.” Geochim. Cosmochim. Acta 67, 1129–

1143. https://doi.org/10.1016/S0016-7037(00)01203-6

Anagnostou, E., Sherrell, R.M., Gagnon, A., LaVigne, M., Field, M.P., McDonough, W.F., 2011. Seawater nutrient and carbonate ion concentrations recorded as P/Ca, Ba/Ca, and U/Ca in the deep-sea coral Desmophyllum dianthus. Geochim. Cosmochim. Acta 75, 2529–2543. https://doi.org/10.1016/j.gca.2011.02.019

Barker, S., Greaves, M., Elderfield, H., 2003. A study of cleaning procedures used for foraminiferal Mg/Ca paleothermometry. Geochemistry, Geophys. Geosystems 4, 8407. https://doi.org/10.1029/2003GC000559

Bates, S.L., Hendry, K.R., Pryer, H. V., Kinsley, C.W., Pyle, K.M., Woodward, E.M.S., Horner, T.J., 2017. Barium isotopes reveal role of ocean circulation on barium cycling in the Atlantic. Geochim. Cosmochim. Acta 204, 286–299. https://doi.org/10.1016/J.GCA.2017.01.043

Bice, K.L., Layne, G.D., Dahl, K., 2005. Application of secondary ion mass spectrometry to the determination of Mg/Ca in rare, delicate, or altered planktonic foraminifera: Examples from the Holocene, Paleogene, and Cretaceous. Geochemistry, Geophys. Geosystems 6, Q12P07. https://doi.org/10.1029/2005GC000974

Bishop, J.K.B., 1988. The barite-opal-organic carbon association in oceanic particulate matter. Nature 332, 341–343. https://doi.org/10.1038/332341a0

Bostock, H.C., Mikaloff Fletcher, S.E., Williams, M.J.M., 2013. Estimating carbonate parameters from hydrographic data for the intermediate and deep waters of the Southern Hemisphere oceans. Biogeosciences 10, 6199–6213. https://doi.org/10.5194/bg-10-6199-2013

Bower, A., Furey, H., 2017. Iceland-Scotland Overflow Water transport variability through the Charlie-Gibbs Fracture Zone and the impact of the North Atlantic Current. J. Geophys. Res. Ocean. 122, 6989–7012. https://doi.org/10.1002/2017JC012698

Burke, A., Robinson, L.F., 2012. The Southern Ocean's Role in Carbon Exchange During the Last Deglaciation. Science. 335, 557–561. https://doi.org/10.1126/science.1208163

Burke, A., Robinson, L.F., McNichol, A.P., Jenkins, W.J., Scanlon, K.M., Gerlach, D.S., 2010. Reconnaissance dating: A new radiocarbon method applied to assessing the temporal distribution of Southern Ocean deep-sea corals. Deep. Res. Part I Oceanogr. Res. Pap. 57, 1510–1520. https://doi.org/10.1016/j.dsr.2010.07.010

Cairns, S.D., Kitahara, M. V., 2012. An illustrated key to the genera and subgenera of the

Recent azooxanthellate Scleractinia (Cnidaria, Anthozoa), with an attached glossary. Zookeys 227, 1–47. https://doi.org/10.3897/zookeys.227.3612

Cantrell, C.A., 2008. Technical Note: Review of methods for linear least-squares fitting of data and application to atmospheric chemistry problems. Atmos. Chem. Phys. Atmos. Chem. Phys. 8, 5477–5487. https://doi.org/10.5194/acpd-8-6409-2008

Cardinal, D., Savoye, N., Trull, T.W., André, L., Kopczynska, E.E., Dehairs, F., 2005. Variations of carbon remineralisation in the Southern Ocean illustrated by the Baxs proxy. Deep. Res. Part I Oceanogr. Res. Pap. 52, 355–370. https://doi.org/10.1016/j.dsr.2004.10.002

Carritt, D.E., Carpenter, J.H., 1966. Comparison and evaluation of currently employed modifications of the Winkler method for determining dissolved oxygen in sea water. A NASCO Report. J. Mar. Res. 24, 286–318.

Case, D.H., Robinson, L.F., Auro, M.E., Gagnon, A.C., 2010. Environmental and biological controls on Mg and Li in deep-sea scleractinian corals. Earth Planet. Sci. Lett. 300, 215–225. https://doi.org/10.1016/j.epsl.2010.09.029

Chan, L.H., Drummond, D., Edmond, J.M., Grant, B., 1977. On the barium data from the Atlantic GEOSECS expedition. Deep. Res. 24, 613–649. https://doi.org/10.1016/0146-6291(77)90505-7

Chen, T.Y., Robinson, L.F., Burke, A., Southon, J., Spooner, P., Morris, P.J., Ng, H.C., 2015. Synchronous centennial abrupt events in the ocean and atmosphere during the last deglaciation. Science. 349, 1537–1541. https://doi.org/10.1126/science.aac6159

Cheng, H., Adkins, J., Edwards, L.R., Boyle, E.A., 2000. U-Th dating of deep-sea corals. Geochim. Cosmochim. Acta 64, 2401–2416. https://doi.org/10.1016/S0016-7037(99)00422-6

Cohen, A.L., McConnaughey, T.A., 2003. Geochemical perspectives on coral mineralization. Rev. Mineral. Geochemistry 54, 151–187. https://doi.org/10.2113/0540151

Collier, R., Edmond, J., 1984. The trace element geochemistry of marine biogenic particulate matter. Prog. Oceanogr. 13, 113–199. https://doi.org/10.1016/0079-6611(84)90008-9

Dehairs, F., Chesselet, R., Jedwab, J., 1980. Discrete suspended particles of barite and the barium cycle in the open ocean. Earth Planet. Sci. Lett. 49, 528–550. https://doi.org/10.1016/0012-821X(80)90094-1

Dietzel, M., Gussone, N., Eisenhauer, A., 2004. Co-precipitation of Sr2+ and Ba2+ with

aragonite by membrane diffusion of CO2 between 10 and 50 oC. Chem. Geol. 203, 139–151. https://doi.org/10.1016/j.chemgeo.2003.09.008

Dymond, J., Suess, E., Lyle, M., 1992. Barium in Deep-Sea Sediment: A Geochemical Proxy for Paleoproductivity. Paleoceanography 7, 163–181. https://doi.org/10.1029/92PA00181

Gaetani, G.A., Cohen, A.L., 2006. Element partitioning during precipitation of aragonite from seawater: A framework for understanding paleoproxies. Geochim. Cosmochim. Acta 70, 4617–4634. https://doi.org/10.1016/j.gca.2006.07.008

Gaetani, G.A., Cohen, A.L., Wang, Z., Crusius, J., 2011. Rayleigh-based, multi-element coral thermometry: A biomineralization approach to developing climate proxies. Geochim. Cosmochim. Acta 75, 1920–1932. https://doi.org/10.1016/j.gca.2011.01.010

Gagnon, A.C., Adkins, J.F., Fernandez, D.P., Robinson, L.F., 2007. Sr/Ca and Mg/Ca vital effects correlated with skeletal architecture in a scleractinian deep-sea coral and the role of Rayleigh fractionation. Earth Planet. Sci. Lett. 261, 280–295. https://doi.org/10.1016/j.epsl.2007.07.013

Ganeshram, R.S., François, R., Commeau, J., Brown-Leger, S.L., 2003. An experimental investigation of barite formation in seawater. Geochim. Cosmochim. Acta 67, 2599–2605. https://doi.org/10.1016/S0016-7037(03)00164-9

Gonneea, M.E., Cohen, A.L., DeCarlo, T.M., Charette, M.A., 2017. Relationship between water and aragonite barium concentrations in aquaria reared juvenile corals. Geochim. Cosmochim. Acta 209, 123–134. https://doi.org/10.1016/j.gca.2017.04.006

Hathorne, E.C., Gagnon, A., Felis, T., Adkins, J., Asami, R., Boer, W., Caillon, N., Case, D., Cobb, K.M., Douville, E., Demenocal, P., Eisenhauer, A., Garbe-Schönberg, D., Geibert, W., Goldstein, S., Hughen, K., Inoue, M., Kawahata, H., Kölling, M., Cornec, F.L., Linsley, B.K., McGregor, H. V., Montagna, P., Nurhati, I.S., Quinn, T.M., Raddatz, J., Rebaubier, H., Robinson, L., Sadekov, A., Sherrell, R., Sinclair, D., Tudhope, A.W., Wei, G., Wong, H., Wu, H.C., You, C.F., 2013. Interlaboratory study for coral Sr/Ca and other element/Ca ratio measurements. Geochemistry, Geophys. Geosystems 14, 3730–3750. https://doi.org/10.1002/ggge.20230

Hemsing, F., Hsieh, Y.-T., Bridgestock, L., Spooner, P.T., Robinson, L.F., Frank, N., Henderson, G.M., 2018. Barium isotopes in cold-water corals. Earth Planet. Sci. Lett. 491, 183–192. https://doi.org/10.1016/J.EPSL.2018.03.040

Hendry, K.R., Georg, R.B., Rickaby, R.E.M., Robinson, L.F., Halliday, A.N., 2010. Deep

ocean nutrients during the Last Glacial Maximum deduced from sponge silicon isotopic compositions. Earth Planet. Sci. Lett. 292, 290–300. https://doi.org/10.1016/j.epsl.2010.02.005

Holcomb, M., DeCarlo, T.M., Schoepf, V., Dissard, D., Tanaka, K., McCulloch, M., 2015. Cleaning and pre-treatment procedures for biogenic and synthetic calcium carbonate powders for determination of elemental and boron isotopic compositions. Chem. Geol. 398, 11–21. https://doi.org/10.1016/j.chemgeo.2015.01.019

Hönisch, B., Allen, K.A., Russell, A.D., Eggins, S.M., Bijma, J., Spero, H.J., Lea, D.W., Yu, J., 2011. Planktic foraminifers as recorders of seawater Ba/Ca. Mar. Micropaleontol. 79, 52–57. https://doi.org/10.1016/j.marmicro.2011.01.003

Hoppema, M., Dehairs, F., Navez, J., Monnin, C., Jeandel, C., Fahrbach, E., de Baar, H.J.W., 2010. Distribution of barium in the Weddell Gyre: Impact of circulation and biogeochemical processes. Mar. Chem. 122, 118–129. https://doi.org/10.1016/j.marchem.2010.07.005

Jacquet, S.H.M., Dehairs, F., Elskens, M., Savoye, N., Cardinal, D., 2007. Barium cycling along WOCE SR3 line in the Southern Ocean. Mar. Chem. 106, 33–45. https://doi.org/10.1016/j.marchem.2006.06.007

Jacquet, S.H.M., Dehairs, F., Savoye, N., Obernosterer, I., Christaki, U., Monnin, C., Cardinal, D., 2008. Mesopelagic organic carbon remineralization in the Kerguelen Plateau region tracked by biogenic particulate Ba. Deep. Res. Part II Top. Stud. Oceanogr. 55, 868–879. https://doi.org/10.1016/j.dsr2.2007.12.038

Jeandel, C., Dupre, B., Lebaron, G., Monnin, C., Minster, J.F., 1996. Longitudinal distributions of dissolved barium, silica and alkalinity in the western and southern Indian Ocean. Deep. Res. Part I Oceanogr. Res. Pap. 43, 1–31. https://doi.org/10.1016/0967-0637(95)00098-4

Jones, S.M., Murton, B.J., Fitton, J.G., White, N.J., Maclennan, J., Walters, R.L., 2014. A joint geochemical-geophysical record of time-dependent mantle convection south of Iceland. Earth Planet. Sci. Lett. 386, 86–97. https://doi.org/10.1016/j.epsl.2013.09.029

LaVigne, M., Grottoli, A.G., Palardy, J.E., Sherrell, R.M., 2016. Multi-colony calibrations of coral Ba/Ca with a contemporaneous in situ seawater barium record. Geochim. Cosmochim. Acta 179, 203–216. https://doi.org/10.1016/j.gca.2015.12.038

LaVigne, M., Hill, T.M., Spero, H.J., Guilderson, T.P., 2011. Bamboo coral Ba/Ca: Calibration of a new deep ocean refractory nutrient proxy. Earth Planet. Sci. Lett. 312,

506–515. https://doi.org/10.1016/j.epsl.2011.10.013

Lea, D.W., Boyle, E.A., 1993. Determination of carbonate-bound barium in foraminifera and corals by isotope dilution plasma-mass spectrometry. Chem. Geol. 103, 73–84. https://doi.org/10.1016/0009-2541(93)90292-Q

Lea, D.W., Pak, D.K., Paradis, G., 2005. Influence of volcanic shards on foraminiferal Mg/Ca in a core from the Galápagos region. Geochemistry, Geophys. Geosystems 6, Q11P04. https://doi.org/10.1029/2005GC000970

Levitus, S., Boyer, T.P., 1994. World Ocean Atlas 1994 Vol. 4: Temperature, Number 4.

Limbeck, A., Galler, P., Bonta, M., Bauer, G., Nischkauer, W., Vanhaecke, F., 2015. Recent advances in quantitative LA-ICP-MS analysis: challenges and solutions in the life sciences and environmental chemistry. Anal. Bioanal. Chem. 407, 6593–6617. https://doi.org/10.1007/s00216-015-8858-0

Margolin, A.R., Robinson, L.F., Burke, A., Waller, R.G., Scanlon, K.M., Roberts, M.L., Auro, M.E., van de Flierdt, T., 2014. Temporal and spatial distributions of cold-water corals in the Drake Passage: Insights from the last 35,000 years. Deep. Res. Part II Top. Stud. Oceanogr. 99, 237–248. https://doi.org/10.1016/j.dsr2.2013.06.008

McConnaughey, T., 1989. 13C and 18O isotopic disequilibrium in biological carbonates: I. Patterns. Geochim. Cosmochim. Acta 53, 151–162. https://doi.org/10.1016/0016-7037(89)90282-2

Mitsuguchi, T., Uchida, T., Matsumoto, E., Isdale, P.J., Kawana, T., 2001. Variations in Mg/Ca, and Sr/Ca ratios of coral skeletons with chemical treatments: Implications for carbonate geochemistry. Geochim. Cosmochim. Acta 65, 2865–2874. https://doi.org/10.1016/S0016-7037(01)00626-3

Montagna, P., McCulloch, M., Douville, E., Lopez Correa, M., Trotter, J., Rodolfo-Metalpa, R., Dissard, D., Ferrier-Pages, C., Frank, N., Freiwald, A., Goldstein, S., Mazzoli, C., Reynaud, S., Ruggeberg, A., Russo, S., Taviani, M., 2014. Li/Mg systematics in scleractinian corals: Calibration of the thermometer. Geochim. Cosmochim. Acta 132, 288–310. https://doi.org/10.1016/j.gca.2014.02.005

Ni, Y., Foster, G.L., Bailey, T., Elliott, T., Schmidt, D.N., Pearson, P., Haley, B., Coath, C., 2007. A core top assessment of proxies for the ocean carbonate system in surface-dwelling foraminifers. Paleoceanography 22, PA3212. https://doi.org/10.1029/2006PA001337

Nozaki, Y., 1997. A fresh look at element distribution in the North Pacific Ocean. Eos, Trans. Am. Geophys. Union 78, 221–221. https://doi.org/10.1029/97EO00148

Okai, T., Suzuki, A., Kawahata, H., Terashima, S., Imai, N., 2002. Preparation of a new Geological Survey of Japan geochemical reference material: Coral JCp-1. Geostand. Newsl. 26, 95–99. https://doi.org/10.1111/j.1751-908X.2002.tb00627.x

Pierrot, D., Lewis, E., Wallace, D.W.R., 2006. MS Excel program developed for CO2 system calculations. ORNL/CDIAC-105a. Carbon Dioxide Inf. Anal. Center, Oak Ridge Natl. Lab. US Dep. Energy, Oak Ridge, Tennessee. https://doi.org/10.3334/CDIAC/otg.CO2SYS_XLS_CDIAC105a

Rae, J.W.B., Foster, G.L., Schmidt, D.N., Elliott, T., 2011. Boron isotopes and B/Ca in benthic foraminifera: Proxies for the deep ocean carbonate system. Earth Planet. Sci. Lett. 302, 403–413. https://doi.org/10.1016/j.epsl.2010.12.034

Roberts, J.M., 2006. Reefs of the Deep: The Biology and Geology of Cold-Water Coral Ecosystems. Science. 312, 543–547. https://doi.org/10.1126/science.1119861

Robinson, L.F., 2014. RRS James Cook Cruise JC094, October 13–November 30 2013, Tenerife-Trinidad. TROPICS, Tracing Oceanic Processes using Corals and Sediments. Reconstructing abrupt Changes in Chemistry and Circulation of the Equatorial Atlantic Ocean.

Robinson, L.F., Adkins, J.F., Frank, N., Gagnon, A.C., Prouty, N.G., Brendan Roark, E., de Flierdt, T. van, 2014. The geochemistry of deep-sea coral skeletons: A review of vital effects and applications for palaeoceanography. Deep. Res. Part II Top. Stud. Oceanogr. 99, 184–198. https://doi.org/10.1016/j.dsr2.2013.06.005

Rosenthal, Y., Field, M.P., Sherrell, R.M., 1999. Precise determination of element/calcium ratios in calcareous samples using sector field inductively coupled plasma mass spectrometry. Anal. Chem. 71, 3248–3253. https://doi.org/10.1021/ac981410x

Rosenthal, Y., Perron-Cashman, S., Lear, C.H., Bard, E., Barker, S., Billups, K., Bryan, M., Delaney, M.L., DeMenocal, P.B., Dwyer, G.S., Elderfield, H., German, C.R., Greaves, M., Lea, D.W., Marchitto, T.M., Pak, D.K., Paradis, G.L., Russell, A.D., Schneider, R.R., Scheiderich, K., Stott, L., Tachikawa, K., Tappa, E., Thunell, R., Wara, M., Weldeab, S., Wilson, P.A., 2004. Interlaboratory comparison study of Mg/Ca and Sr/Ca measurements in planktonic foraminifera for paleoceanographic research. Geochemistry, Geophys. Geosystems 5, Q04D09. https://doi.org/10.1029/2003GC000650

Shen, G.T., Boyle, E.A., 1988. Determination of lead, cadmium and other trace metals in annually-banded corals. Chem. Geol. 67, 47–62. https://doi.org/10.1016/0009-2541(88)90005-8

Sinclair, D.J., Williams, B., Risk, M., 2006. A biological origin for climate signals in corals - Trace element “vital effects” are ubiquitous in Scleractinian coral skeletons. Geophys. Res. Lett. 33, L17707. https://doi.org/10.1029/2006GL027183

Spooner, P.T., Chen, T., Robinson, L.F., Coath, C.D., 2016a. Rapid uranium-series age screening of carbonates by laser ablation mass spectrometry. Quat. Geochronol. 31, 28–39. https://doi.org/10.1016/j.quageo.2015.10.004

Spooner, P.T., Guo, W., Robinson, L.F., Thiagarajan, N., Hendry, K.R., Rosenheim, B.E., Leng, M.J., 2016b. Clumped isotope composition of cold-water corals: A role for vital effects? Geochim. Cosmochim. Acta 179, 123–141. https://doi.org/10.1016/j.gca.2016.01.023

Sternberg, E., Tang, D., Ho, T.Y., Jeandel, C., Morel, F.M.M., 2005. Barium uptake and adsorption in diatoms. Geochim. Cosmochim. Acta 69, 2745–2752. https://doi.org/10.1016/j.gca.2004.11.026

Stroobants, N., Dehairs, F., Goeyens, L., Vanderheijden, N., Van Grieken, R., 1991. Barite formation in the Southern Ocean water column. Mar. Chem. 35, 411–421. https://doi.org/10.1016/S0304-4203(09)90033-0

Sundby, S., Drinkwater, K.F., Kjesbu, O.S., 2016. The North Atlantic Spring-Bloom System—Where the Changing Climate Meets the Winter Dark. Front. Mar. Sci. 3, 28. https://doi.org/10.3389/fmars.2016.00028

Thiagarajan, N., Subhas, A. V., Southon, J.R., Eiler, J.M., Adkins, J.F., 2014. Abrupt pre-Bølling–Allerød warming and circulation changes in the deep ocean. Nature 511, 75–78. https://doi.org/10.1038/nature13472

Tudhope, A.W., Lea, D.W., Shimmield, G.B., Chilcott, C.P., Head, S., 1996. Monsoon climate and Arabian sea Coastal Upwelling Recorded in Massive Corals from Southern Oman. Palaios 11, 347–361. https://doi.org/10.2307/3515245

van Beek, P., Sternberg, E., Reyss, J.L., Souhaut, M., Robin, E., Jeandel, C., 2009. 228Ra/226Ra and 226Ra/Ba ratios in the Western Mediterranean Sea: Barite formation and transport in the water column. Geochim. Cosmochim. Acta 73, 4720–4737. https://doi.org/10.1016/j.gca.2009.05.063

van de Flierdt, T., Robinson, L.F., Adkins, J.F., 2010. Deep-sea coral aragonite as a recorder for the neodymium isotopic composition of seawater. Geochim. Cosmochim. Acta 74, 6014–6032. https://doi.org/10.1016/j.gca.2010.08.001

Watanabe, T., Minagawa, M., Oba, T., Winter, A., 2001. Pretreatment of coral aragonite for Mg and Sr analysis: Implications for coral thermometers. Geochem. J. 35, 265–269. https://doi.org/10.2343/geochemj.35.265

York, D., Evensen, N.M., Martínez, M.L., De Basabe Delgado, J., 2004. Unified equations for the slope, intercept, and standard errors of the best straight line. Am. J. Phys. 72, 367. https://doi.org/10.1119/1.1632486

Cleaning step	Fe/Ca (µmol/mol)	Err. (2 S.E.)	Ba/Ca (µmol/mol)	Err. (2 S. E.)
NBP0805-TB10-Dp-3				
2	2.05	0.07	12.46	0.13
3	1.67	0.06	12.62	0.13
4	1.26	0.04	12.30	0.13
5	0.89	0.03	12.36	0.13
6	1.99	0.07	12.67	0.13
7	1.00	0.03	12.38	0.13
CE0806-Dr18-1				
1	44.05	1.45	7.33	0.08
2	41.92	1.38	7.35	0.08
4	19.6	0.65	7.18	0.08
6	9.15	0.3	7.21	0.08
7	4.26	0.14	7.20	0.08

Table 1: Elemental ratios of corals measured after chemical cleaning. Cleaning steps follow the descriptions in the text: 1) Shipboard washes and lab-based physical cleaning only, 2) 15 min US in milli-q and powdering; 3) 15 min US oxidising solution; 4) 2 min perchloric acid rinse; 5) 15 min US in milli-q; 6) 1 min US in 0.2 % HNO_3; 7) as 3; 8) 20 min US reducing solution. Every sample was replicated once and the ratios here are the mean of the two replicates of each cleaning stage.

Extended calibration of cold-water coral Ba/Ca using multiple genera and co-located measurements of dissolved barium concentration: List of figures

1. Maps of a) Drake Passage and b) tropical Atlantic sample sites. Red points indicate coral collection sites named as follows: a) BB, Burdwood Bank; SS, Sars Seamount; b) GS, Gramberg Seamount; VS, Vayda Seamount; VFZ, Vema Fracture Zone; KS, Knipovich Seamount; CS, Carter Seamount. Grey points indicate locations where $[Ba]_{sw}$ has been measured in seawater samples. Plotted using Ocean Data View.

2. Typical solitary cold-water coral skeleton of the genus Caryophyllia, labelled with the macroscale features and redrawn after Cairns and Kitahara (2012), and a schematic cross section through a coral septum illustrating the microscale features COCs and TDs.

3. Measured a) Temperature, b) Salinity and c) $[Ba]_{sw}$ (nmol/kg) depth profiles near each sample site. Samples from CTD casts are shown with black outline. Samples from Niskin bottles aboard the ROV are shown with no outline. Coral sample depths are shown along the sides of panel (b). Estimates of water properties at the depths of coral collection are based on extrapolation of the data in the relevant curve to that depth. In some cases, temperature and salinity were measured as the corals were collected (Spooner et al. 2016b).

4. Impact of chemical cleaning on the measured Ba/Ca (a,b) and Fe/Ca (c,d) of powders from the corals NBP1103-TB10-Dp-3 (Desmophyllum; a,c) and CE0806-Dr18-1 (Desmophyllum; b,d). Cleaning stages are numbered as follows: 1) shipboard washing and lab-based physical cleaning only, 2) 15 min US in milli-q; 3) 15 min US oxidising solution; 4) 2 min perchloric acid rinse; 5) 15 min US in milli-q; 6) 1 min US in 0.2 % HNO_3; 7) as 3; 8) 20 min US reducing solution. Full details of the oxidising and reducing solutions can be found in Section 2.4. Dashed lines indicate the means of the measurements. Where no error bars can be seen, errors are smaller than the data points.

5. 2 standard deviations of Ba/Ca ratios taken from different size fractions for the corals NBP0805-TB04-Big Beauty (10 samples per size fraction) and CE0806-DR04A-1 (5 samples per size fraction).

6. Ba/Ca in coral skeletons versus dissolved seawater Ba concentration ($[Ba]_{sw}$). A linear least squares lines of best fit is drawn through the data (solid line) with confidence intervals (grey area, 2 S.E.) included. The dashed line indicates the weighted bivariate fit as discussed in Section 3.3. Vertical error bars are based on the 2 S.D. of repeat Ba/Ca measurements on the standard materials. Horizontal error bars are estimates of the $[Ba]_{sw}$ uncertainty. Where no vertical error bars can be seen, errors are smaller than the data points.

7. Reconstruction uncertainties on the dissolved seawater Ba concentration ($[Ba]_{sw}$) when estimated from cold-water coral Ba/Ca using the calibration from data in this study. Both the 95 % and 68 % uncertainty intervals are indicated.

8. a) Dissolved Ba in seawater ($[Ba]_{sw}$) versus seawater temperature (T) and b) salinity (S) for the sample sites from which corals were collected during this study. c) Coral skeleton Ba/Ca ratio versus T and d) S for the same sample sites.

9. Measured Ba/Ca in coral skeletons versus dissolved seawater Ba concentration ($[Ba]_{sw}$) in multiple studies. Data from this study and Hemsing et al. (2018) have been corrected as described in the text, and the linear least squares fit through all the data from the two studies (averaged where the same coral was measured in both studies) is shown with confidence intervals. Linear least squares lines of best fit are also shown for the data from each other study individually.

10. Calculated D_{Ba} versus $[Ba]_{sw}$ for the data presented in this study. A linear least squares fit is plotted through the data for illustrative purposes.

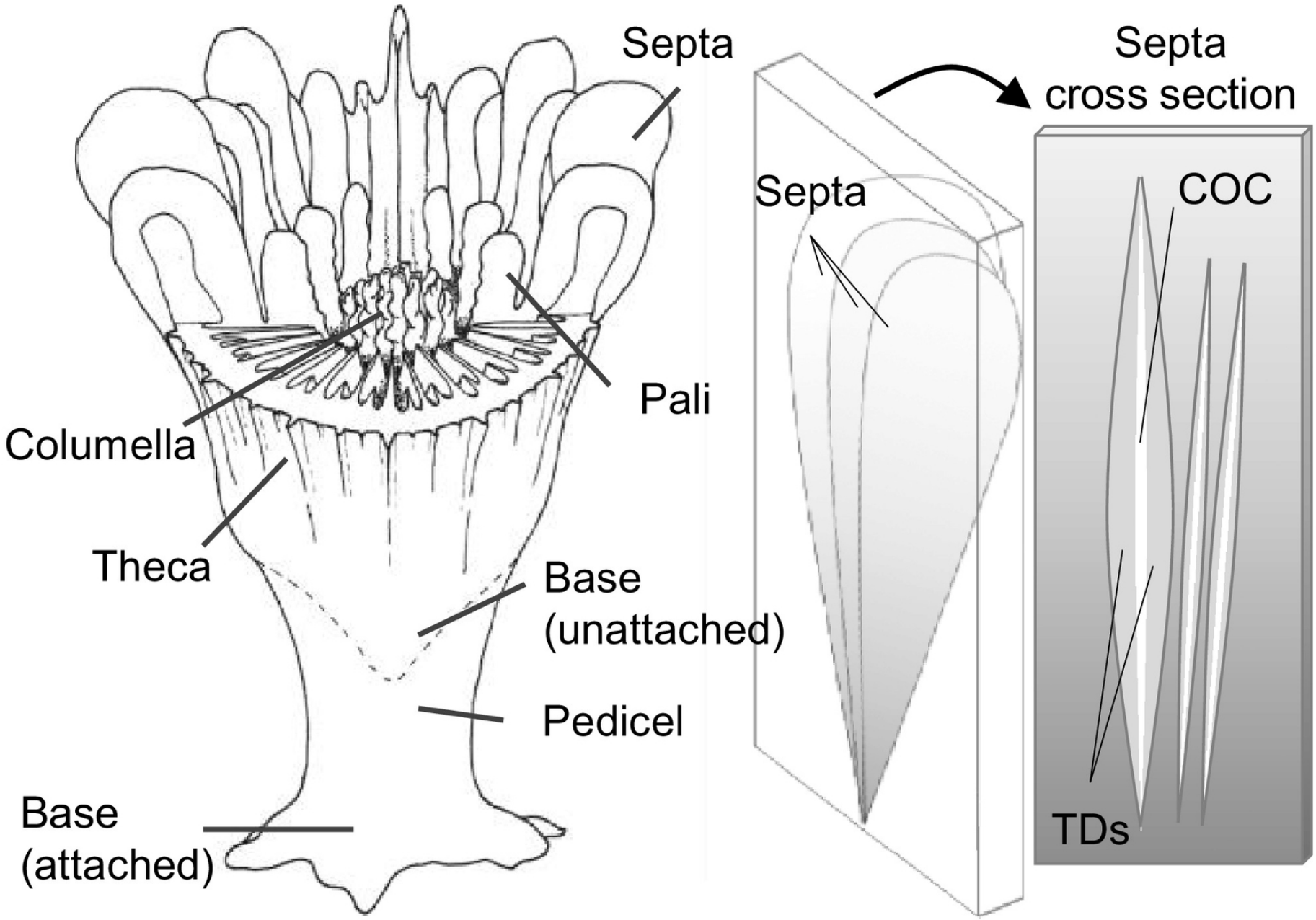
Septa
Pali
Columella
Theca
Base
(unattached)
Pedicel
Base
(attached)
Septa
cross section
Septa
COC
TDs

Figure 1

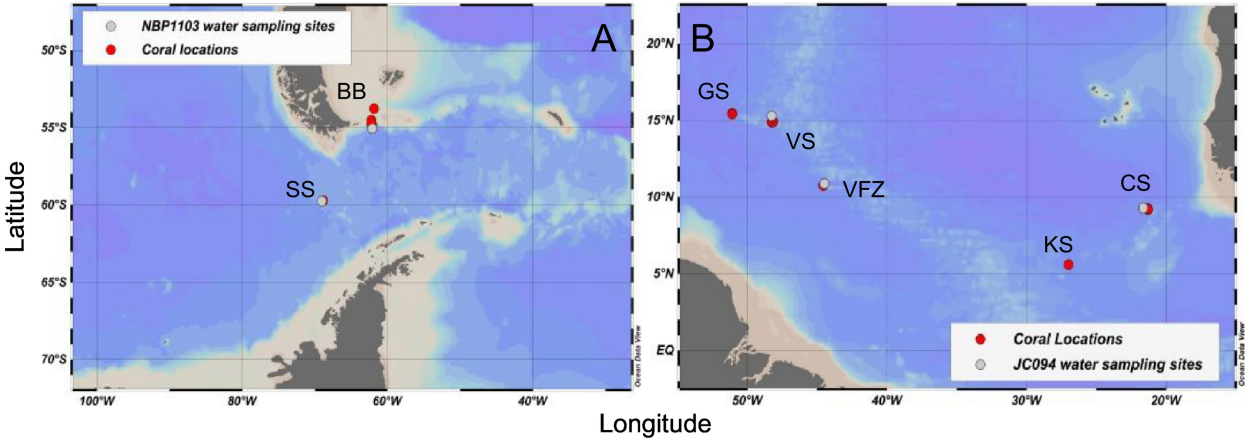
NBP1103 water sampling sites
Coral locations
A
BB
SS
50°S
55°S
60°S
65°S
70°S
100°W
80°W
60°W
40°W
B
GS
VS
VFZ
CS
KS
20°N
15°N
10°N
5°N
EQ
50°W
40°W
30°W
20°W
Coral Locations
JC094 water sampling sites
Latitude
Longitude

Figure 2

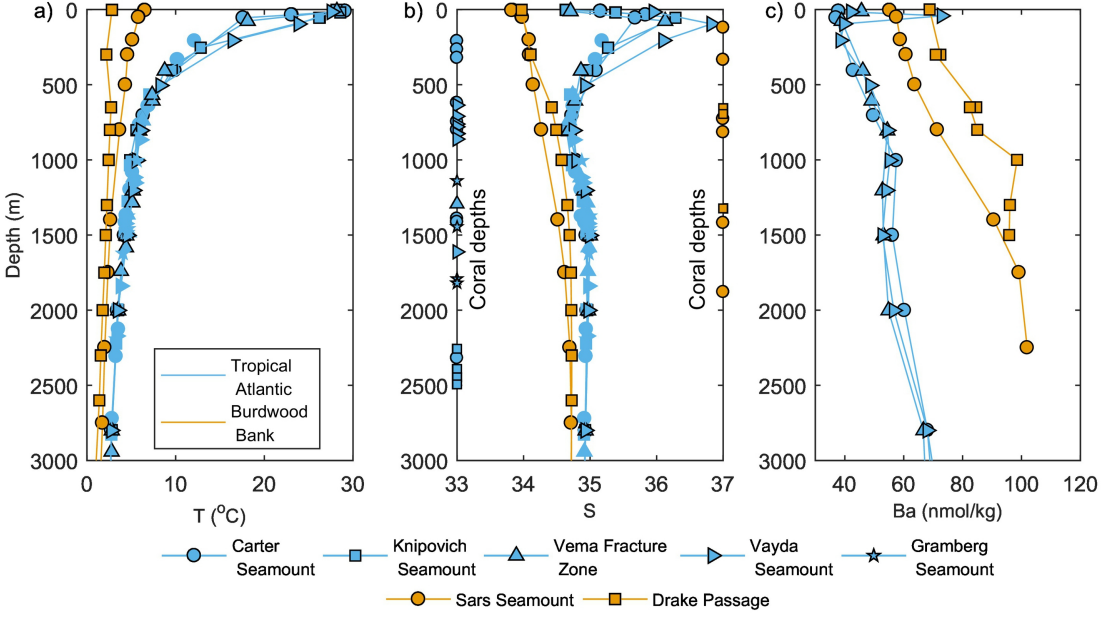
a)
b)
c)
Depth (m)
T (°C)
S
Ba (nmol/kg)
Coral depths
Coral depths
Tropical Atlantic
Burdwood Bank
Carter Seamount
Knipovich Seamount
Vema Fracture Zone
Vayda Seamount
Gramberg Seamount
Sars Seamount
Drake Passage

Figure 3

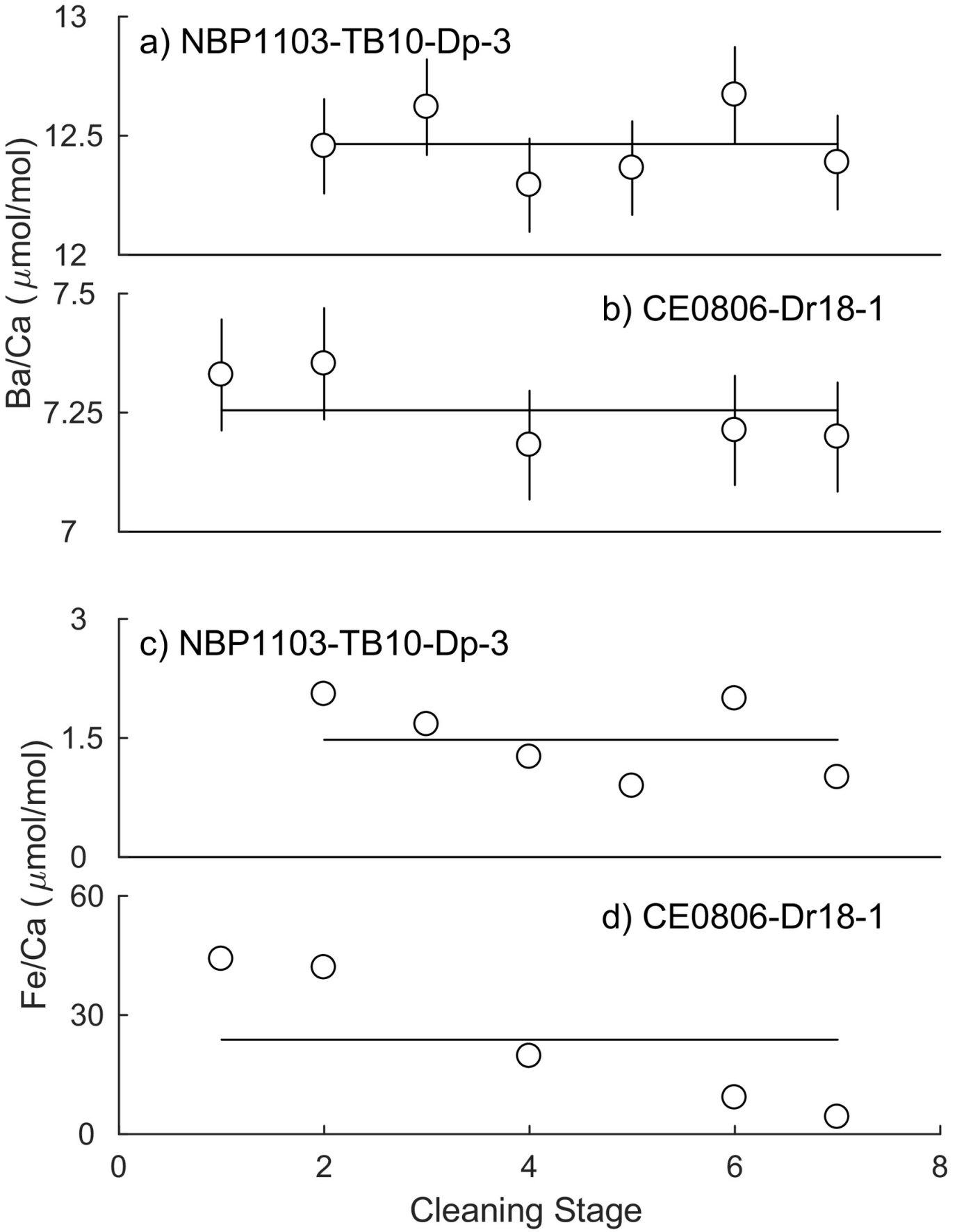
a) NBP1103-TB10-Dp-3
b) CE0806-Dr18-1
c) NBP1103-TB10-Dp-3
d) CE0806-Dr18-1
Ba/Ca (μmol/mol)
Fe/Ca (μmol/mol)
Cleaning Stage
13
12.5
12
7.5
7.25
7
3
1.5
0
60
30
0
0
2
4
6
8

Figure 4

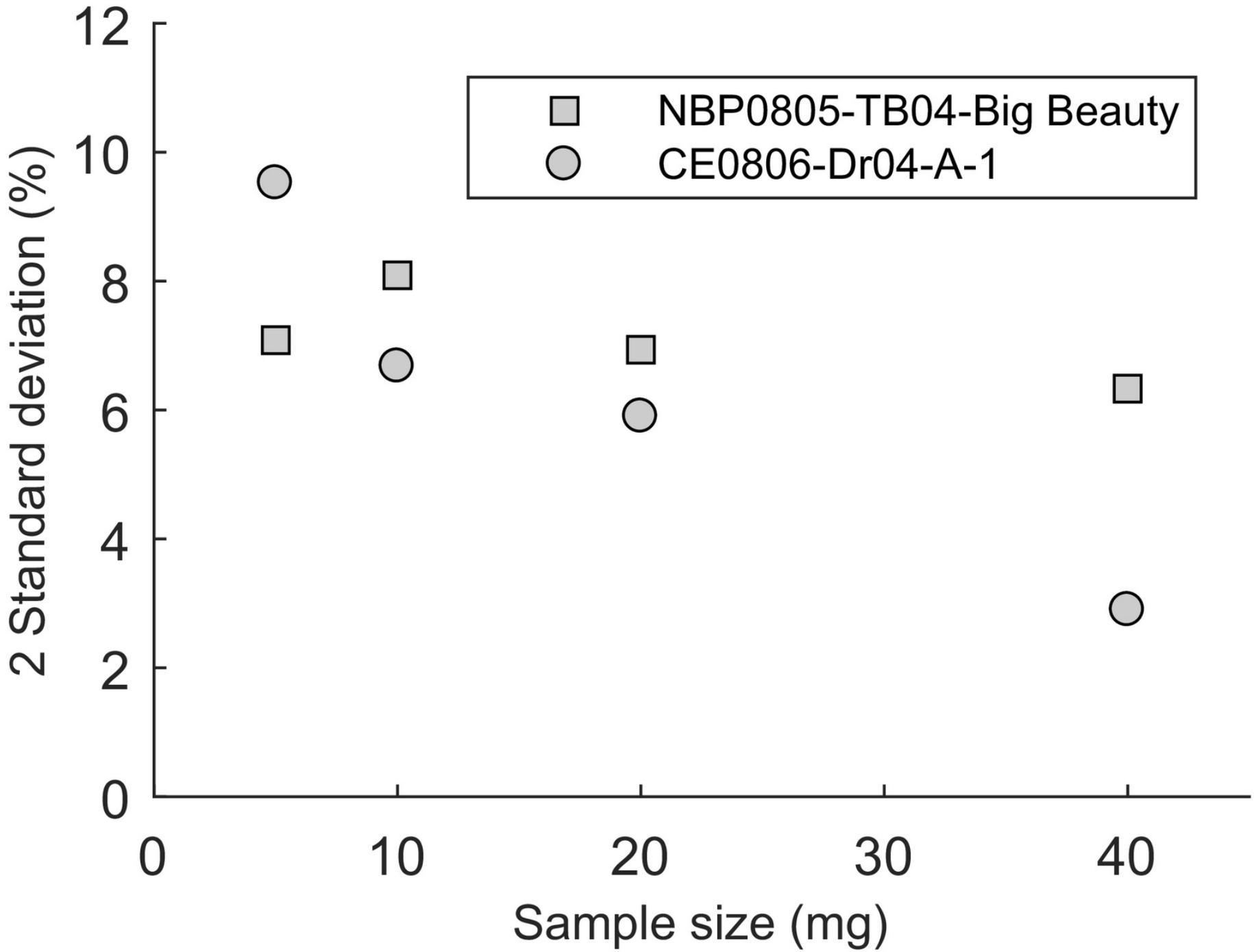
12
10
8
6
4
2
0
2 Standard deviation (%)
0
10
20
30
40
Sample size (mg)
NBP0805-TB04-Big Beauty
CE0806-Dr04-A-1

Figure 5

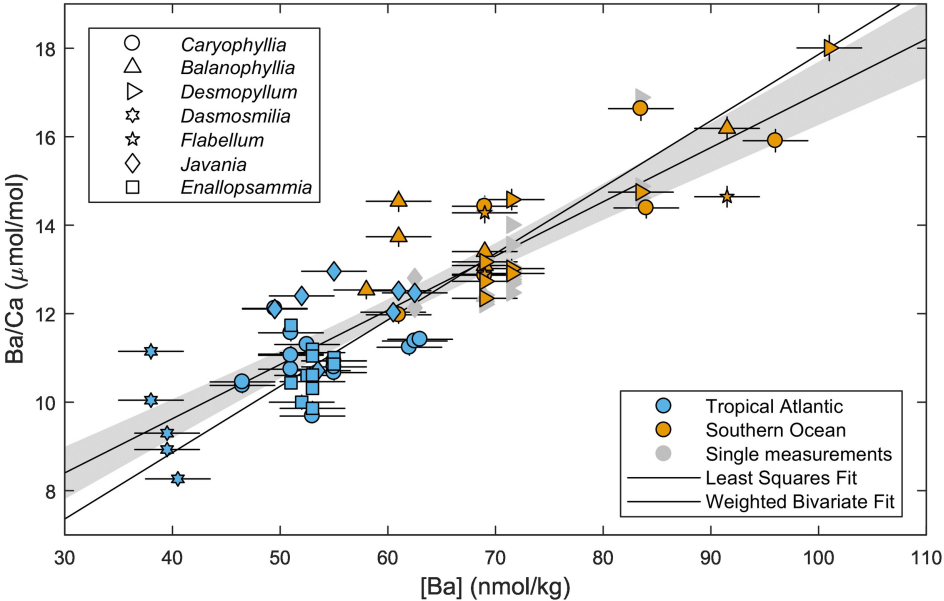
Caryophyllia
Balanophyllia
Desmopyllum
Dasmosmilia
Flabellum
Javania
Enallopsammia
Tropical Atlantic
Southern Ocean
Single measurements
Least Squares Fit
Weighted Bivariate Fit
Ba/Ca (μmol/mol)
[Ba] (nmol/kg)
8
10
12
14
16
18
30
40
50
60
70
80
90
100
110

Figure 6

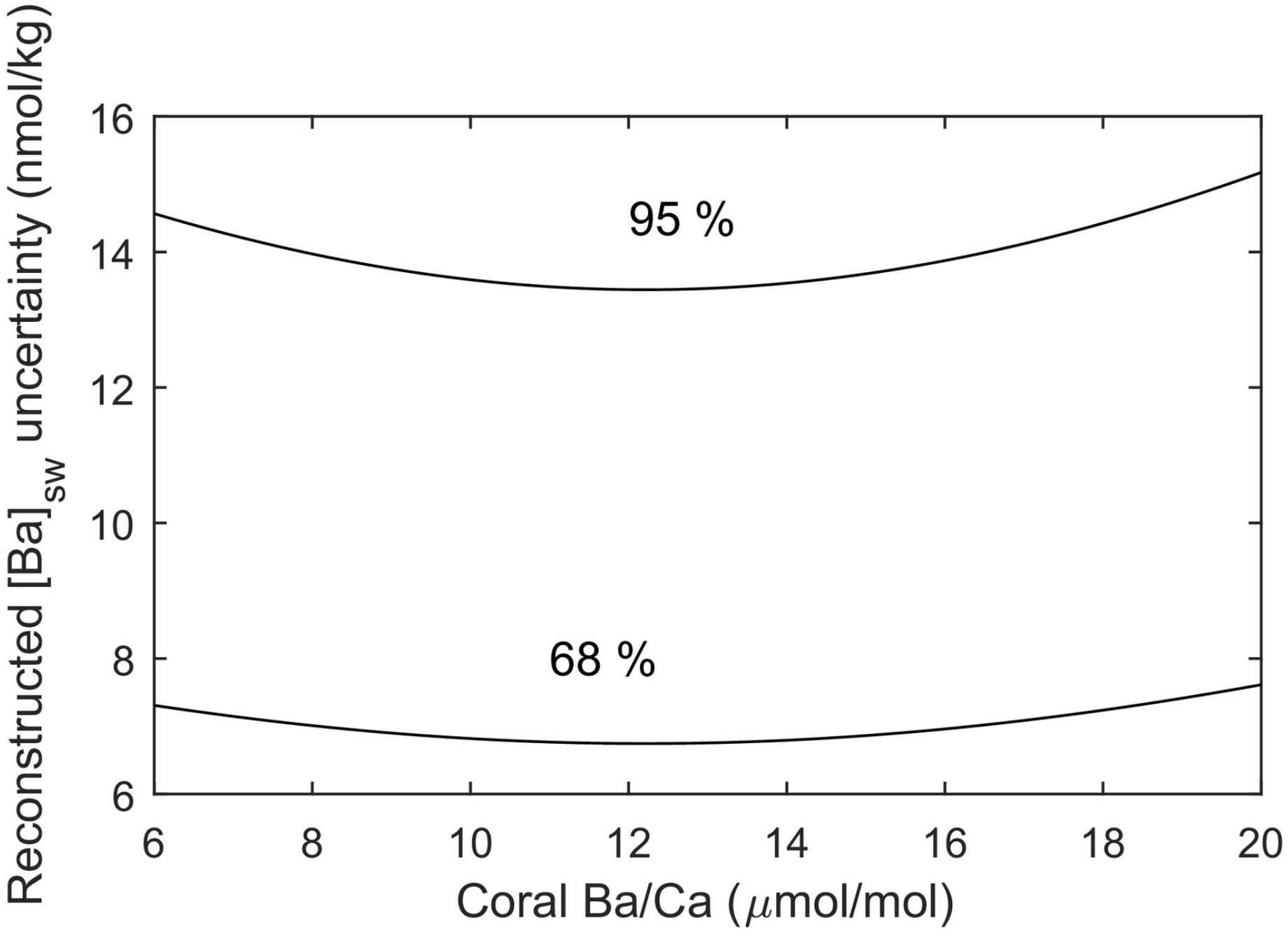
Reconstructed [Ba]sw uncertainty (nmol/kg)
16
14
12
10
8
6
95 %
68 %
6
8
10
12
14
16
18
20
Coral Ba/Ca (μmol/mol)

Figure 7

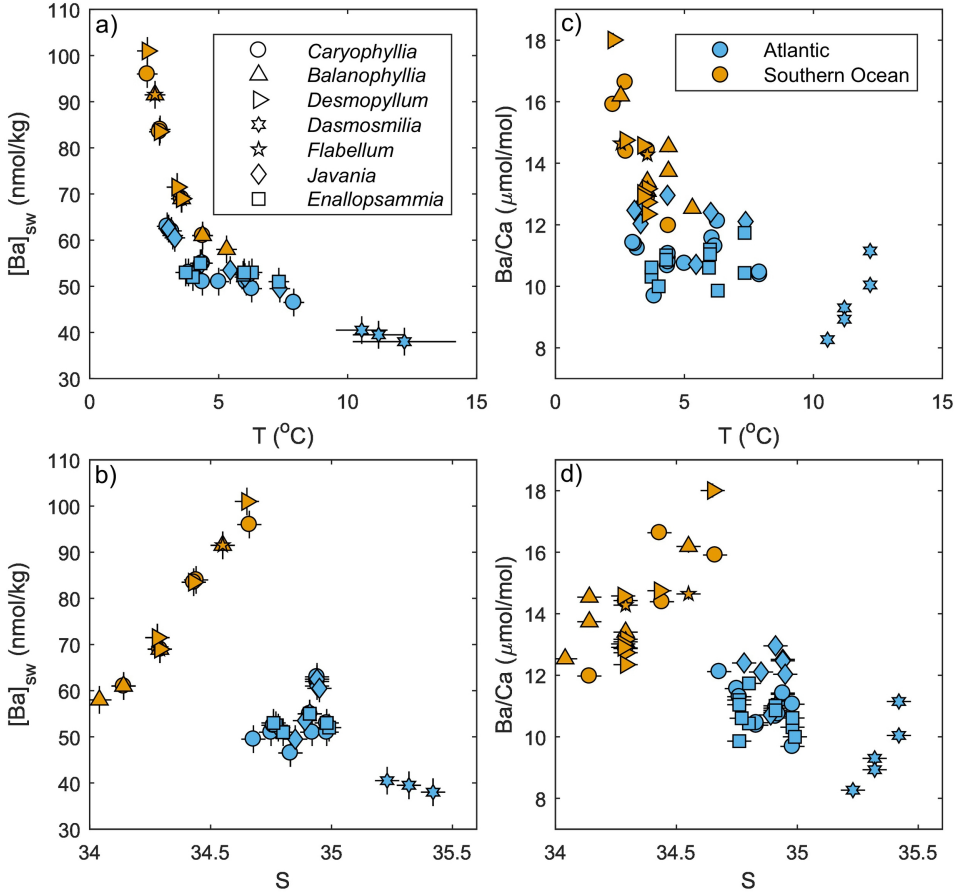
a)
c)
b)
d)
Caryophyllia
Balanophyllia
Desmopyllum
Dasmosmilia
Flabellum
Javania
Enallopsammia
Atlantic
Southern Ocean
[Ba]sw (nmol/kg)
Ba/Ca (μmol/mol)
T (°C)
S

Figure 8

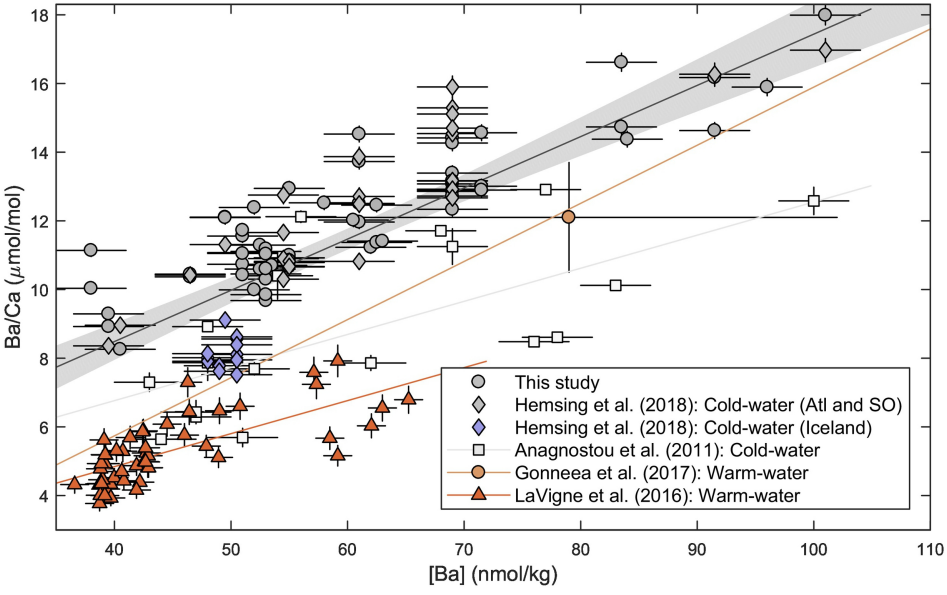
Ba/Ca (μmol/mol)
[Ba] (nmol/kg)
This study
Hemsing et al. (2018): Cold-water (Atl and SO)
Hemsing et al. (2018): Cold-water (Iceland)
Anagnostou et al. (2011): Cold-water
Gonneea et al. (2017): Warm-water
LaVigne et al. (2016): Warm-water

Figure 9

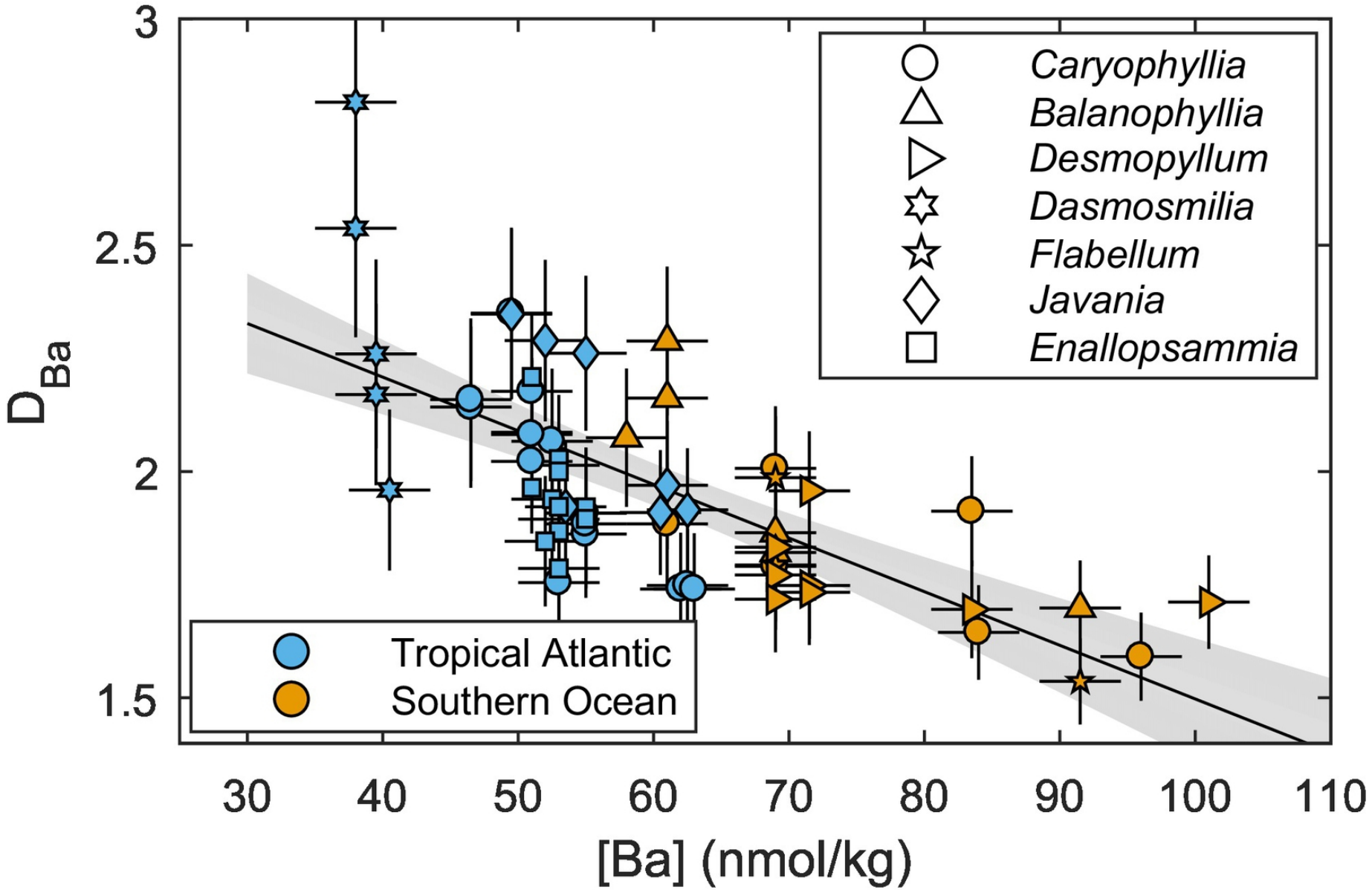
3
2.5
2
1.5
D_{Ba}
30
40
50
60
70
80
90
100
110
[Ba] (nmol/kg)
Caryophyllia
Balanophyllia
Desmopyllum
Dasmosmilia
Flabellum
Javania
Enallopsammia
Tropical Atlantic
Southern Ocean

Figure 10